Arresting Classical Many-Body Chaos by Kinetic Constraints

Aydin Deger,[1,*] Sthitadhi Roy,[2,3,4,†] and Achilleas Lazarides[1,‡]
[1]*Interdisciplinary Centre for Mathematical Modelling and Department of Mathematical Sciences, Loughborough University, Loughborough, Leicestershire LE11 3TU, United Kingdom*
[2]*International Centre for Theoretical Sciences, Tata Institute of Fundamental Research, Bengaluru 560089, India*
[3]*Rudolf Peierls Centre for Theoretical Physics, Oxford University, Parks Road, Oxford OX1 3PU, United Kingdom*
[4]*Physical and Theoretical Chemistry, Oxford University, South Parks Road, Oxford OX1 3QZ, United Kingdom*

(Received 16 March 2022; accepted 19 September 2022; published 12 October 2022)

We investigate the effect of kinetic constraints on classical many-body chaos in a translationally invariant Heisenberg spin chain using a classical counterpart of the out-of-time-ordered correlator (OTOC). The strength of the constraint drives a "dynamical phase transition" separating a delocalized phase, where the classical OTOC propagates ballistically, from a localized phase, where the OTOC does not propagate at all and the entire system freezes. This is unexpected given that all spin configurations are dynamically connected to each other. We show that localization arises due to the dynamical formation of frozen islands, contiguous segments of spins immobile due to the constraints, dominating over the melting of such islands.

DOI: 10.1103/PhysRevLett.129.160601

Ergodicity lies at the heart of bridging microscopic theories of many-body systems to macroscopic thermodynamic descriptions of such systems via their statistical mechanics [1]. Much of this is underpinned by the notion of chaos captured by the butterfly effect—an infinitesimal local change in the initial condition, a wingbeat of the proverbial butterfly, can amplify exponentially and spread ballistically in spacetime to effect drastic changes in the global state at later times, such as cause a tornado in a different part of the world [2–4].

Recently, the out-of-time-ordered correlator (OTOC) has emerged as a prominent diagnostic for many-body quantum chaos [5–15]. Defined as $\mathcal{O}(x,t) = -\langle [W(x,t), V(0,0)]^2 \rangle$, it measures the effect on a local operator W at position x and time t of perturbing the system with an operator V at $x = 0$ and $t = 0$. A classical counterpart of the OTOC was developed to characterize spatiotemporal chaos in classical many-body systems [16–20]. It quantifies how the degrees of freedom in two copies of a system dynamically decorrelate in spacetime due to an infinitesimal local difference in their initial conditions. For chaotic systems, the OTOC or its classical counterpart has a ballistically propagating front, which might be sharp or broaden diffusively.

Although ergodicity is generally considered the default, it is by now clear that there exist several classes of systems where ergodicity is broken, often strongly and robustly. Such systems therefore violate conventional statistical mechanics and thermodynamics; fundamental questions thus emerge about their universal, macroscopic descriptions. Telltale signatures of ergodicity breaking include long, often divergent, relaxation timescales, absence of thermalization, suppressed transport, and specific to quantum systems, arrested growth of entanglement. All of these above phenomena can be loosely brought under the umbrella of (quasi)localization of classical or quantum information.

Among the earliest examples of ergodicity breaking, perhaps the most significant ones are structural and spin glasses, which become nonergodic usually at low temperatures [21–27]. A key ingredient in these systems is the presence of quenched random disorder. At the same time, disorder in low-dimensional quantum systems is also understood to cause strong ergodicity breaking, even at infinite temperatures, via Anderson localization [28,29] in

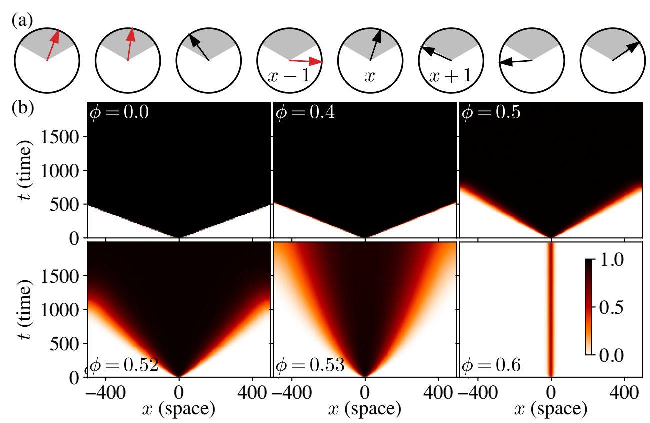

FIG. 1. (a) Schematic of the constrained spin chain. The red spins are frozen as *both* their neighbors lie inside the spherical sector (gray shade) which has a polar angle $\phi\pi$, whereas the black spins are free to evolve. (b) The classical OTOCs and decorrelators $\langle D(x,t) \rangle$ as color maps in spacetime for several values of ϕ. Note the rapid slowing down of the light cone with ϕ near $\phi_c \approx 0.53$, above which the light cone is fully arrested.

noninteracting and many-body localization [30–32] in interacting systems.

However, disorder is not a prerequisite for ergodicity breaking. In translation-invariant systems, kinetic constraints have long emerged as one of the most prominent pathways to classical glassy behavior at low temperatures [33–39]. Also in quantum systems, at infinite temperatures, kinetic constraints have been shown to result in slow relaxation [40–42] and stabilize a many-body localized phase as well [43]. This motivates our investigation of the fate of classical many-body chaos, characterized by the classical OTOC, in the presence of local kinetic constraints and at infinite temperatures.

Remarkably, we find that, as a function of a parameter ϕ quantifying the strength of the constraints, the dynamics undergoes a sharp dynamical phase transition between an ergodic phase, where the OTOC spreads out ballistically, and a nonergodic phase, where spreading is completely arrested—see Fig. 1 for a summary. As the constraints in our model keep the entire configuration space dynamically connected, localization is *not* due to fragmentation of configuration space [44–47].

Instead, localization occurs because the distribution of waiting times (the time the front of the classical OTOC waits at a site before moving onto the next) above some critical constraint strength acquires a heavy enough power-law tail that the mean waiting time diverges (Fig. 2).

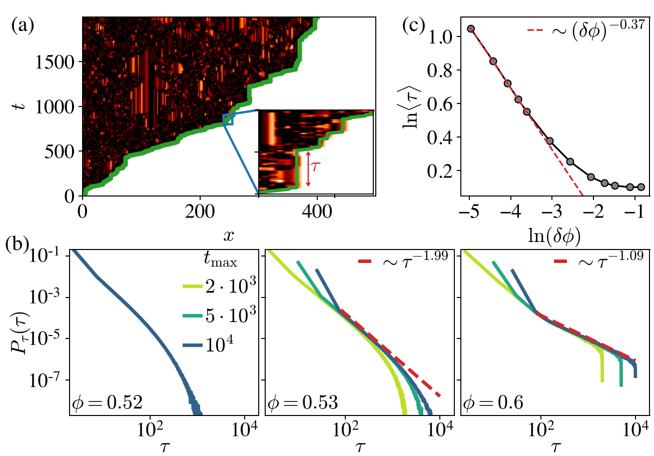

FIG. 2. (a) $D(x,t)$ for a randomly chosen initial condition along with the trajectory of the front $x_F^R(t)$, extracted using Eq. (6), shown in green. Inset: a small spacetime portion enlarged, as well as the definition of τ. Data for $\phi = 0.53$ and $\eta = 0.01$. (b) Distributions of the waiting time $P_\tau(\tau)$ for three different ϕ, each for three different maximum simulation times $t_{\max}$. While the distributions are converged with $t_{\max}$ and not tailed in the delocalized phase, they have heavy power-law tails in the localized phase that persist for longer τ for larger $t_{\max}$ and have exponents such that the mean $\langle\tau\rangle$ is divergent. (c) The numerical data suggest that $\langle\tau\rangle$ diverges as a power law with $\delta\phi = \phi_c - \phi$ and $\phi_c \approx 0.525(5)$. All statistics accumulated over 5×10^5 initial conditions.

We link this distribution to the broadening of the front caused by the constraints and provide insight into the mechanism of localization by showing that melting of initially frozen regions happens locally, starting at the edges of the islands, while formation of frozen islands can occur anywhere in the system. Whether the entire system becomes localized is then a question of the lifetimes of these islands, which diverges at the same ϕ as the mean waiting time (Fig. 3).

Further evidence for localization is provided by the fact that, in the ergodic phase, islands of initially frozen spins (due to the constraints) melt from the edges and eventually the entire system becomes active. In the localized phase, not only is melting of these initial frozen islands arrested, but the system also dynamically develops several frozen islands with divergent lifetimes, which eventually proliferate and freeze the entire system.

For simplicity, we strip our model of all conservation laws (including energy) so that in the unconstrained limit ($\phi = 0$), the OTOC has a sharp front with no broadening. In the presence of constraints but in the ergodic phase the distribution of waiting times broadens the front diffusively.

For concreteness, we consider a periodically driven classical Heisenberg chain of length L with periodic boundaries described by the Hamiltonian,

$$\mathcal{H}(t) = \begin{cases} \sum_{x=-L/2}^{L/2} (J S_x^z S_{x+1}^z + h S_x^z), & t \in [nT, (n+\frac{1}{2})T) \\ \sum_{x=-L/2}^{L/2} g S_x^x, & t \in [(n+\frac{1}{2})T, (n+1)T) \end{cases}, \tag{1}$$

where the spin at site x is a three-dimensional unit vector $\mathbf{S}_x = (S_x^x, S_x^y, S_x^z)$. Since the model defined in Eq. (1) is time periodic, we consider the dynamics only at stroboscopic times $t = nT$ with integer n. In the presence of kinetic constraints, the stroboscopic evolution of the spins is given by

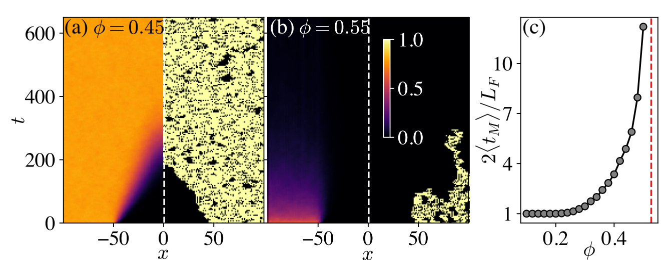

FIG. 3. Melting of an initially frozen island of length $L_F = 100$ in the delocalized phase (a) or lack thereof in the localized phase (b). The plots show a color map of $A_x(t)$ with black denoting frozen spins $A_x(t) \approx 0$ and yellow denoting active with $A_x(t) \approx 1$. In each panel, the left half shows averaged data $\langle A(x,t)\rangle$, whereas the right half shows it for a single initial condition. The data in (c) suggest that the mean melting time t_M, diverges as the critical ϕ_c is approached from the delocalized side. The red dashed line denotes the estimated ϕ_c from the decorrelator data.

$$\mathbf{S}_x[(n+1)T] = \begin{cases} \mathsf{R_x}[gT/2]\mathsf{R_z}[\theta_x(nT)]\mathbf{S}_x(nT); & \Theta_x(nT)=1 \\ \mathbf{S}_x(nT); & \Theta_x(nT)=0 \end{cases}, \tag{2}$$

where $\mathsf{R_z}[\theta_x(nT)]$ denotes a 3D rotation matrix about the z axis by an angle $\theta_x(nT) \equiv [S^z_{x-1}(nT) + S^z_{x+1}(nT) + h]T/2$ and similarly for $\mathsf{R_x}$. The constraints are encoded in the Heaviside step function,

$$\Theta_x(nT) = \Theta[\cos(\pi\phi) - \min(S^z_{x-1}(nT), S^z_{x+1}(nT))]. \tag{3}$$

The form of the constraint implies that a spin at site x is frozen if *both* its neighbors lie inside the spherical sector defined by the polar angle $\pi\phi$; see Fig. 1(a) for a visual schematic. In this sense, it can be considered as the Heisenberg generalization of the Fredrickson-Andersen constraint defined originally for Ising spins [33,34]. Physically, in the context of glassy dynamics, interpreting spins inside (outside) the sector as proxies for (for example) high(low)-density regions in a system where density is the dynamical variable, the constraints forbid dynamics in a region if it is surrounded by dense immobile regions [38]. In what follows, we set $T = 2\pi$, $J = 1$, $h = 0.1$, and $g = 0.4$ without loss of generality.

The classical OTOC is defined by considering two initial conditions $\{\mathbf{S}_{x,A}(t=0)\}$ and $\{\mathbf{S}_{x,B}(t=0)\}$ identical everywhere except at $x = 0$, where they are infinitesimally different,

$$\delta\mathbf{S}_x(0) \equiv \mathbf{S}_{x,A}(0) - \mathbf{S}_{x,B}(0) = \varepsilon\delta_{x,0}[\hat{\mathbf{z}} \times \mathbf{S}_{x,A}(0)]. \tag{4}$$

The classical OTOC, henceforth referred to as the "decorrelator," is then given by [16]

$$D(x,t) = 1 - \mathbf{S}_{x,A}(t) \cdot \mathbf{S}_{x,B}(t). \tag{5}$$

As we are interested in the infinite temperature dynamics of the decorrelator, we average it over several randomly and uniformly chosen initial conditions; we denote the average as $\langle D(x,t)\rangle$ [48] and use $\varepsilon = 10^{-3}$ throughout.

The results for $\langle D(x,t)\rangle$ are shown in Fig. 1(b) for several values of ϕ. For $\phi = 0$, the dynamics is completely unconstrained. Since the system has no conservation laws, we observe a sharp ballistic light cone for $\langle D(x,t)\rangle$, the front of which does not broaden. On increasing ϕ, the constraints come into play and within the "delocalized" phase, while the light cone still has a well-defined butterfly velocity, there is broadening of the front. We shall shortly explain this using the distribution of waiting times. In the vicinity of $\phi_c \approx 0.53$, the light cone slows down while the front broadens significantly. We attribute this slow dynamics with large fluctuations to the fact that we are at or near a dynamical phase transition separating the delocalized and localized phases. The localized phase is evident from the data for $\phi = 0.6$, where the light cone is completely arrested; the front neither propagates nor broadens.

A key ingredient that determines the spatiotemporal profile of the decorrelator is the "waiting time" denoted by τ. This is defined as the time the *front* of the decorrelator waits at x before moving to site $x + \mathrm{sgn}(x)$. The front of the decorrelator is defined as follows. For a fixed time t, the right (left) front, $x_F^{(R/L)}(t)$ is at

$$x_F^{(R/L)}(t) = \max/\min\{x | D(x,t) \geq \eta\}, \tag{6}$$

where $\eta \ll 1$ is an empirically chosen cutoff. A representative trajectory of x_F^R over time is shown in Fig. 2(a), where a series of vertical steps (the length of each being a waiting time τ) is visible. These steps are distributed over spacetime and initial conditions with a distribution P_τ, shown in Fig. 2(b) for various ϕ and simulation times. In the delocalized phase ($\phi = 0.52$), P_τ converges with increasing maximum simulation time $t_{\max}$, decaying faster than any power law and having a finite mean $\langle\tau\rangle = \int^\infty d\tau\, \tau P_\tau(\tau)$. As the system transitions into the localized phase ($\phi = 0.53$ and $\phi = 0.6$), $P_\tau(\tau)$ develops power-law tails, $P_\tau(\tau) \sim \tau^{-\alpha}$. These tails are cut off by $t_{\max}$ but, crucially, extend up to longer τ for larger $t_{\max}$ This suggests that when $t_{\max} \to \infty$ the tail remains a power law all the way to $\tau \to \infty$. For $\phi \geq \phi_c \approx 0.525(5)$, the exponent $\alpha \leq 2$, i.e., the tail of P_τ becomes heavy enough that $\langle\tau\rangle \to \infty$. From the data in Fig. 2(b), we conjecture that, at $\phi = \phi_c$, $\alpha = 2$. The time taken by the front to reach a site at a given x is $\sim x\langle\tau\rangle$, which diverges so that the front gets stuck and the light cone does not spread at all [49]. In Fig. 2(c), we show how $\langle\tau\rangle$ diverges as $\phi \to \phi_c$ from the delocalized side. The data on logarithmic axes show that it diverges as a power law with an exponent $\nu \approx 0.4$ [50].

So far we have established that the constraints (3) induce a "localized" phase, wherein classical many-body chaos as quantified by the decorrelator (5) is completely arrested. We next show that, in fact, the entire system actually freezes in a random spin configuration, which depends on the initial condition, and provide a physical picture for localization.

The mechanism can be understood in terms of "frozen islands": contiguous segments of spins such that $\Theta_x = 0$ [see Eq. (3)] for all of them. All spins in such a segment and the spins immediately on either side have $S^z > \cos(\pi\phi)$; hence they are frozen. During the evolution, such islands can melt (the spins becoming active) progressively inward from the edges of the island. In the delocalized phase, these islands melt at a finite velocity and the entire system becomes active at late times. In the localized phase, new frozen islands appear, proliferating through the entire system such that it freezes into a random configuration. Of course, for any value of ϕ, new frozen islands appear dynamically. However, the crucial difference is that, for $\phi < \phi_c$, these islands quickly melt with timescales that are proportional to the length of the island. On the contrary, for $\phi > \phi_c$, the rate at which new islands appear overwhelms the rate at which they melt, such that the entire system becomes one frozen island.

We next present numerical evidence for this picture. We start with an ensemble of initial conditions with a frozen island of size L_F in the middle and the rest of the spins random. We then define a function $A_x(t) = \Theta[\cos(\pi\phi) - \min(S^z_{x-1}(t), S^z_{x+1}(t))]$, taking a value 1(0) if the spin is active (frozen), and track this dynamically. The results are shown in Fig. 3 and are in agreement with the discussion in the previous paragraph. Furthermore, from the data for a single initial condition, it can be seen that new frozen islands form dynamically in the initially active regions, quickly melt in the delocalized phase, and persist and eventually take over the entire system in the localized phase.

To quantify this further, we define a melting time t_M for each initial condition as the earliest time the spin at $x = 0$ (furthest from the edges of the island) becomes active, $t_M = \min\{t|A_0(t) = 1\}$. In the delocalized phase, since the melting happens at the constant velocity on average, we expect that the average melting time $\langle t_M\rangle \propto L_F$. However, in the localized phase, since the initial frozen island never melts, the spin at site $x = 0$ is never active for any finite t. This is consistent with the apparent divergence of $\langle t_M\rangle$ as $\phi \to \phi_c$ from the delocalized side in Fig. 3(c).

Finally, we discuss the spatiotemporal profile of the decorrelator in the delocalized phase, focusing in particular on the broadening of the front. For $\phi = 0$ there is no broadening, so that any broadening at $\phi \neq 0$ must be due to the constraints. As Fig. 4(a) demonstrates for a representaive value of ϕ, the mean decorrelator for different times can be collapsed onto a scaling function,

$$\langle D(x,t)\rangle = \mathcal{F}\left[\frac{x \mp x_v(t)}{\xi(t)}\right]; \qquad x \gtrless 0. \tag{7}$$

Fitting for each t, Figs. 4(b) and 4(c) show that the parameters $x_v(t) = v_B(\phi)t$ and $\xi(t) = \gamma(\phi)t^{1/2}$, so that the front moves ballistically while broadening diffusively. The broadening is a direct result of the finite width of the distribution P_τ. Defining ℓ as the distance the front moves in a single period, the finite width of P_τ naturally implies that the distribution P_ℓ has a nonzero width. Moreover, since the model is local, ℓ is strictly bounded from above, which means all the moments of P_ℓ are finite. Let us denote the first two moments by $\pm\mu_\ell$ (for the front at $x \gtrless 0$ and with $\mu_\ell > 0$) and σ^2_ℓ, respectively. According to the central limit theorem, the distance moved after t periods, $X_t = \sum_{n=1}^t \ell_n$ with ℓ_n distributed according to P_ℓ, is normally distributed with mean $t\mu_\ell$ and standard deviation $\sqrt{t}\sigma_\ell$. Modeling the decorrelator for a single initial condition by a Heaviside step function $D(x,t) = \Theta(X_t - |x|)$ and averaging over the normal distribution of the X_t, we find

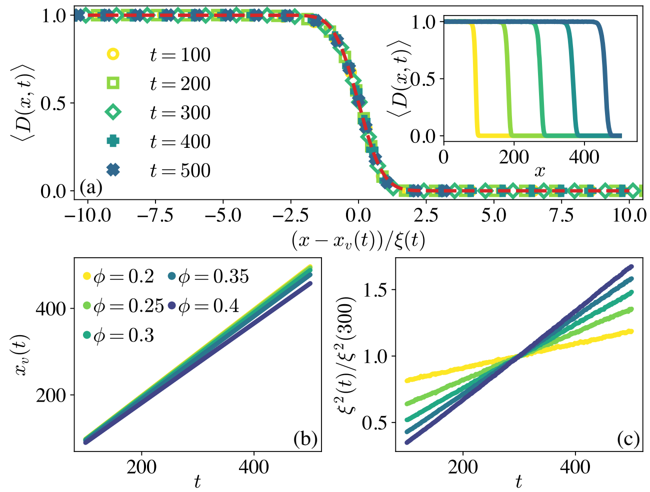

FIG. 4. (a) Collapse of $\langle D(x,t)\rangle$ onto a function $\mathcal{F}[(x - x_v(t))/\xi(t)]$ for $x > 0$ with $\mathcal{F}(y) = \mathrm{erfc}(y)$ denoted by the red dashed line. Inset: raw data. The plots use $\phi = 0.4$. (b) $x_v(t)$ as a function of t for several values of ϕ in the delocalized phase. The linear behavior indicates the presence of a well-defined butterfly velocity $v_B = x_v(t)/t$. (c) $\xi^2(t)$ for the same values of ϕ, rescaled (arbitrarily) with $\xi^2(300)$ for visual clarity. The linear behavior indicates the diffusive broadening of the decorrelator front.

$$\langle D(x,t)\rangle = \frac{1}{2}\mathrm{erfc}\left(\frac{x \mp t\mu_\ell}{\sqrt{2t\sigma^2_\ell}}\right); \qquad x \gtrless 0, \tag{8}$$

so that $v_B(\phi) = \mu_\ell(\phi)$ and $\gamma(\phi) = \sqrt{2}\sigma_\ell(\phi)$. An implication of Eq. (8) is that, on a spacetime ray with velocity v ($x = vt$) outside the light cone, we can write $\langle D(x,t)\rangle \sim \exp[\lambda_v t]$, where $\lambda_v(\phi) \approx -[v - v_B(\phi)]^2/\gamma(\phi)$ is the velocity-dependent Lyapunov exponent [15].

To summarize, we have demonstrated that constrained dynamics can completely arrest classical many-body chaos as measured via the classical counterpart of the OTOC. Our results also provide compelling evidence for a dynamical phase transition, driven by the strength of the constraint, separating a delocalized phase where the classical OTOC spreads ballistically from a localized phase where it does not spread at all. The physical mechanism behind this localization was shown to be that, in the course of the dynamics, frozen islands of spins form and proliferate through the system, freezing it entirely. These islands also form dynamically in the delocalized phase but they quickly melt away. A consequence of the constraint-induced frozen spins is that, as correlations spread in spacetime, they encounter the frozen spins and need to wait until they are dynamically active again. The arrest of spreading is reflected in the distribution of these waiting times acquiring heavy power-law tails in the localized phase.

It is worth emphasizing that our results are general, holding for a variety of systems with and without conservation laws and both in one and two dimensions (see Supplemental Material [51]). The form of the constraint we employ (3) allows for a spin to be active even if just one of its neighbors is not in the cone (i.e., "OR" condition). In this sense, the constraint is weaker than the generalizations of "XOR" or "AND" constraints, where exactly one of the two or both neighbors, respectively, need to be outside the cone for a spin to be active. This therefore suggests that the localized phase will be present for the latter two cases.

While we have established the presence of a transition between an ergodic and a localized phase, its precise nature is a question for future work. In a separate work [52], we discuss how it can be mapped onto a directed percolation problem.

Looking further afield, one may ask what lessons can be learned from this classical problem for constrained quantum dynamics. Amid the fragility of many-body localized phases in disordered quantum systems, particularly in higher dimensions, the emergence of constraints as an effective ingredient for localizing quantum information is significant. This aspect also has important practical implications. Modern day noisy intermediate scale quantum devices simulate dynamics to store, manipulate, and retrieve quantum information [53]. An essential challenge there is scrambling of information accompanied by runaway entropy growth, or heating, of the system. Constraints as a way of mitigating this issue without relying on disorder to break ergodicity is an important and timely development. Our results point to a clear direction for further studies on how to arrest quantum chaos leading to information localization.

We thank Y. Bar Lev, S. Bhattacharjee, and A. Dhar for helpful discussions and A. Smith for a careful reading of the manuscript. A. D. and A. L. acknowledge support via EPSRC Grant No. EP/V012177/1. S. R. acknowledges an ICTS-Simons Early Career Faculty Fellowship via a grant from the Simons Foundation (677895, R. G.) and EPSRC Grant No. EP/S020527/1.

*a.deger@lboro.ac.uk
†sthitadhi.roy@icts.res.in
‡a.lazarides@lboro.ac.uk

[1] L. D. Landau and E. M. Lifshitz, *Statistical Physics: Vol. 5*, 3rd ed. (Butterworth-Heinemann, Oxford, 1980).
[2] E. N. Lorenz, Deterministic nonperiodic flow, J. Atmos. Sci. **20**, 130 (1963).
[3] E. N. Lorenz, *The Essence of Chaos* (University of Washington Press, Seattle, 1995).
[4] E. Lorenz, The Butterfly Effect, in *The Chaos Avant-Garde* (World Scientific, Singapore, 2001), pp. 91–94.
[5] A. I. Larkin and Y. N. Ovchinnikov, Quasiclassical method in the theory of superconductivity, Sov. J. Exp. Theor. Phys. **28**, 1200 (1969).
[6] S. H. Shenker and D. Stanford, Black holes and the butterfly effect, J. High Energy Phys. 03 (2014) 067.
[7] D. A. Roberts and D. Stanford, Diagnosing Chaos Using Four-Point Functions in Two-Dimensional Conformal Field Theory, Phys. Rev. Lett. **115**, 131603 (2015).
[8] J. Maldacena, S. H. Shenker, and D. Stanford, A bound on chaos, J. High Energy Phys. 08 (2016) 106.
[9] B. Swingle, G. Bentsen, M. Schleier-Smith, and P. Hayden, Measuring the scrambling of quantum information, Phys. Rev. A **94**, 040302(R) (2016).
[10] A. Bohrdt, C. B. Mendl, M. Endres, and M. Knap, Scrambling and thermalization in a diffusive quantum many-body system, New J. Phys. **19**, 063001 (2017).
[11] D. J. Luitz and Y. Bar Lev, Information propagation in isolated quantum systems, Phys. Rev. B **96**, 020406(R) (2017).
[12] A. Nahum, S. Vijay, and J. Haah, Operator Spreading in Random Unitary Circuits, Phys. Rev. X **8**, 021014 (2018).
[13] C. W. von Keyserlingk, T. Rakovszky, F. Pollmann, and S. L. Sondhi, Operator Hydrodynamics, Otocs, and Entanglement Growth in Systems without Conservation Laws, Phys. Rev. X **8**, 021013 (2018).
[14] T. Rakovszky, F. Pollmann, and C. W. von Keyserlingk, Diffusive Hydrodynamics of Out-of-Time-Ordered Correlators with Charge Conservation, Phys. Rev. X **8**, 031058 (2018).
[15] V. Khemani, D. A. Huse, and A. Nahum, Velocity-dependent Lyapunov exponents in many-body quantum, semiclassical, and classical chaos, Phys. Rev. B **98**, 144304 (2018).
[16] A. Das, S. Chakrabarty, A. Dhar, A. Kundu, D. A. Huse, R. Moessner, S. S. Ray, and S. Bhattacharjee, Light-Cone Spreading of Perturbations and the Butterfly Effect in a Classical Spin Chain, Phys. Rev. Lett. **121**, 024101 (2018).
[17] T. Bilitewski, S. Bhattacharjee, and R. Moessner, Temperature Dependence of the Butterfly Effect in a Classical Many-Body System, Phys. Rev. Lett. **121**, 250602 (2018).
[18] S. D. Murugan, D. Kumar, S. Bhattacharjee, and S. S. Ray, Many-Body Chaos in Thermalized Fluids, Phys. Rev. Lett. **127**, 124501 (2021).
[19] S.-W. Liu, J. Willsher, T. Bilitewski, J.-J. Li, A. Smith, K. Christensen, R. Moessner, and J. Knolle, Butterfly effect and spatial structure of information spreading in a chaotic cellular automaton, Phys. Rev. B **103**, 094109 (2021).
[20] T. Bilitewski, S. Bhattacharjee, and R. Moessner, Classical many-body chaos with and without quasiparticles, Phys. Rev. B **103**, 174302 (2021).
[21] J. H. Gibbs and E. A. DiMarzio, Nature of the glass transition and the glassy state, J. Chem. Phys. **28**, 373 (1958).
[22] J. Jäckle, Models of the glass transition, Rep. Prog. Phys. **49**, 171 (1986).
[23] M. Mézard and G. Parisi, Statistical physics of structural glasses, J. Phys. Condens. Matter **12**, 6655 (2000).
[24] S. F. Edwards and P. W. Anderson, Theory of spin glasses, J. Phys. F **5**, 965 (1975).
[25] D. Sherrington and S. Kirkpatrick, Solvable Model of a Spin-Glass, Phys. Rev. Lett. **35**, 1792 (1975).
[26] K. Binder and A. P. Young, Spin glasses: Experimental facts, theoretical concepts, and open questions, Rev. Mod. Phys. **58**, 801 (1986).
[27] M. Mezard, G. Parisi, and M. Virasoro, *Spin Glass Theory and Beyond* (World Scientific, Singapore, 1986).

[28] P. W. Anderson, Absence of diffusion in certain random lattices, Phys. Rev. **109**, 1492 (1958).

[29] P. A. Lee and T. V. Ramakrishnan, Disordered electronic systems, Rev. Mod. Phys. **57**, 287 (1985).

[30] R. Nandkishore and D. A. Huse, Many-body localization and thermalization in quantum statistical mechanics, Annu. Rev. Condens. Matter Phys. **6**, 15 (2015).

[31] F. Alet and N. Laflorencie, Many-body localization: An introduction and selected topics, C.R. Phys. **19**, 498 (2018).

[32] D. A. Abanin, E. Altman, I. Bloch, and M. Serbyn, Colloquium: Many-body localization, thermalization, and entanglement, Rev. Mod. Phys. **91**, 021001 (2019).

[33] G. H. Fredrickson and H. C. Andersen, Kinetic Ising Model of the Glass Transition, Phys. Rev. Lett. **53**, 1244 (1984).

[34] G. H. Fredrickson and H. C. Andersen, Facilitated kinetic Ising models and the glass transition, J. Chem. Phys. **83**, 5822 (1985).

[35] J. Jäckle and S. Eisinger, A hierarchically constrained kinetic Ising model, Z. Phys. B **84**, 115 (1991).

[36] P. Sollich and M. R. Evans, Glassy Time-Scale Divergence and Anomalous Coarsening in a Kinetically Constrained Spin Chain, Phys. Rev. Lett. **83**, 3238 (1999).

[37] P. Sollich and M. R. Evans, Glassy dynamics in the asymmetrically constrained kinetic Ising chain, Phys. Rev. E **68**, 031504 (2003).

[38] F. Ritort and P. Sollich, Glassy dynamics of kinetically constrained models, Adv. Phys. **52**, 219 (2003).

[39] J. P. Garrahan, P. Sollich, and C. Toninelli, Kinetically constrained models, in *Dynamical Heterogeneities in Glasses, Colloids, and Granular Media*, edited by L. Berthier, G. Biroli, J.-P. Bouchaud, L. Cipelletti, and W. van Saarloos (Oxford University Press, Oxford, 2011).

[40] M. van Horssen, E. Levi, and J. P. Garrahan, Dynamics of many-body localization in a translation-invariant quantum glass model, Phys. Rev. B **92**, 100305(R) (2015).

[41] Z. Lan, M. van Horssen, S. Powell, and J. P. Garrahan, Quantum Slow Relaxation and Metastability Due to Dynamical Constraints, Phys. Rev. Lett. **121**, 040603 (2018).

[42] N. Pancotti, G. Giudice, J. I. Cirac, J. P. Garrahan, and M. C. Bañuls, Quantum East Model: Localization, Nonthermal Eigenstates, and Slow Dynamics, Phys. Rev. X **10**, 021051 (2020).

[43] S. Roy and A. Lazarides, Strong ergodicity breaking due to local constraints in a quantum system, Phys. Rev. Res. **2**, 023159 (2020).

[44] S. Pai, M. Pretko, and R. M. Nandkishore, Localization in Fractonic Random Circuits, Phys. Rev. X **9**, 021003 (2019).

[45] V. Khemani, M. Hermele, and R. Nandkishore, Localization from Hilbert space shattering: From theory to physical realizations, Phys. Rev. B **101**, 174204 (2020).

[46] P. Sala, T. Rakovszky, R. Verresen, M. Knap, and F. Pollmann, Ergodicity Breaking Arising from Hilbert Space Fragmentation in Dipole-Conserving Hamiltonians, Phys. Rev. X **10**, 011047 (2020).

[47] J. Feldmeier and M. Knap, Critically Slow Operator Dynamics in Constrained Many-Body Systems, Phys. Rev. Lett. **127**, 235301 (2021).

[48] As shown in Ref. [16], on canonical quantization of the Poisson brackets $\langle D(x,t)\rangle \to -(\varepsilon^2/\hbar^2)\mathrm{Tr}[[\hat{\mathbf{S}}_x(t), \hat{\mathbf{z}}\cdot\hat{\mathbf{S}}_0(0)]^2]$ which is nothing but the quantum OTOC.

[49] Strictly speaking, this divergence rules out the ballistic spreading of the front. Subsequent results on melting of an initially frozen island (Fig. 3) provides evidence for the complete arrest of the light cone.

[50] A systematic study of the critical behavior incorporating finite-size and finite-time effects is beyond the scope and interest of this work.

[51] See Supplemental Material at http://link.aps.org/supplemental/10.1103/PhysRevLett.129.160601 for results of the time independent Hamiltonian in one spatial dimension and Floquet model on a square lattice in two spatial dimensions.

[52] A. Deger, A. Lazarides, and S. Roy, Constrained dynamics and directed percolation, arXiv:2206.07724.

[53] J. Preskill, Quantum computing in the NISQ era and beyond, Quantum **2**, 79 (2018).